Preliminary report on LBNL 2019 inter-laboratory comparison for laboratories submitting scattering glazing data to the CGDB

Jacob C. Jonsson[1], Helen Rose Wilson[2], Maryna Bilokur[1]
[1]Lawrence Berkeley National Laboratory
and
[2]Fraunhofer ISE

Windows and Envelope Materials Group
Building Technology Department
Building Technology and Urban Systems Division
Energy Technologies Area

September 14, 2021

Disclaimer

Abstract

An inter-laboratory comparison was organized to validate measurement methods for diffuse glazing included in NFRC 300[1] and 301[2]. Several levels of characterization was carried out, starting with precharacterization of samples by the manufacturers to quantify the homogeneity between samples in each sample set. Each participant received a set of samples for which they carried out a full characterization.

The sample set contained 4 homogeneous samples with isotropic scattering, a diffuse interlayer, a fritted glass with low-e on the fritted side, a diffuse applied film on low-iron glass, and an acid-etched glass. In addition samples with with larger scale surface inhomogeneity were included despite not being officially covered by the method.

Comparison of individual participants with averaged results suggest an increase in tolerances compared to specular products. The issues were studied in detail and presented as an argument to loosen the tolerance. The controls and procedures put in place to harmonize haze measurement between spheres with different geometry showed some promise but not sufficient to get great agreement for normal-normal results from all different sphere geometries.

A method for importing and simulating layers described by direct and diffuse transmittance and reflectance was implemented in the Berkley Lab WINDOWS program. Testing of the implementation show that the program is working as intended, and also give some indication on the impact of limiting the wavelength band from full to condensed.

1 Introduction

Optical characterization of diffuse glazing have for a long time been limited to speciality labs that built their own equipment to handle the measurements. With the introduction of a commercially available integrating sphere it became easier for optical labs to perform these measurements accurately and repeatedly.

National Fenestration Rating Council (NFRC) formed a task group in 2015 that investigated the accuracy of this commercially available accessory. That preliminary work showed promising results which resulted in updating the NFRC 300 and 301 measurement standards used by NFRC to cover a procedure how to measure these products.

An inter-laboratory comparison (ILC) was organized to verify the procedures, as well as showing that participating laboratories are getting accurate results. The task group had discussed allowing for a greater tolerance for the values of diffuse properties as these properties are by nature more complicated to measure. However, a proposal to guess new tolerances before an ILC had been carried out was considered ill-informed and the documents were written without any mention of treating properties of diffuse samples differently.

Participation with good results in this ILC is a requirement for laboratories to be approved for submission of spectral data for diffuse glazing to the CGDB.

Additional experimental findings on use of emissometers for measurement of thermal IR properties and calculation of visible haze from these measurements were touched upon in this work.

A new data format to handle the optical results was defined and a way to import the data into WINDOW 7.8 was implemented. Testing of the WINDOW 7.8 implementation was carried out.

This preliminary report focuses on precharacterization results and showing the average of the submitted data with the participating laboratories to allow for CGDB submissions in 2020. Only a small minority of the participants, a total of 5 labs, were able to prioritize this activity due to restrictions posed by the Covid-19 virus.

1.1 Nomenclature

There are multiple naming conventions when discussing diffuse measurements of reflectance and transmittance. For window and glass materials there most prevalent are described here. Ideally we would be strict and use the terms defined in NFRC 300, but when multiple words exist they are included here for educational purposes. The reason for condensed descriptions is typically that only a narrow subset of properties are being described in a certain context, e.g. how for specular glass it is common to only say reflectance and transmittance, rather than the more complete terms normal-normal transmittance and near-normal-near-normal reflectance.

The most descriptive is to combine incident distribution with outgoing distribution, e.g. *direct-diffuse* which would correspond to direct incident light and diffuse outgoing

light. There are at least five different distribution descriptors that work for both incident and outgoing distribution:

Direct In theory it is light described by a ray with a point-like cross section propagating in a single direction. In practice it is a beam collimated beam that might be focused with a narrow cone of angles with a cross section that that is greater than zero, e.g. 10mm x18mm for a Perkin-Elmer Lambda 1050 instrument. Sometimes direct is used a shorthand for normal (e.g. for an instrument where normal is the only possible incidence angle).

Diffuse Light that is scattered over the hemisphere. There is a nuance here between theory and experiment that is sometimes ignored. In experiments the specular component is defined by a solid angle and the diffuse component is defined as the light scattered outside that solid angle. But in theory light can be scattered in the forward direction, e.g. in a bulk-scattering medium light can end up propagating in the forward direction after multiple interactions. When comparing experiment and theory in such situation it can be helpful to designate the measured component as *diffuse only*.

Hemispherical The collection of all light distributed over the hemisphere. The combination of both direct and diffuse light.

Normal Direct light normal to the surface of the sample. The normal direction is defined as zero when describing angle of incidence. Shorter to say than to specify the angle of the direct light and common in most measurement instruments as well as energy performance metrics e.g. SHGC.

Near-normal A more descriptive label high-lighting that reflectance is commonly measure at near normal, typically less than 10 degree angle of incidence. It is common that transmittance is measured at normal angle of incidence, and reflectance at near-normal. Something that is typically fine but has led to issues for samples with strong interference patterns and negligible absorption (where measuring the transmittance at the same angle of incidence as the reflectance is required to avoid the sum of reflectance and transmittance being greater than 1 for some wavelengths).

When working with an instrument that only measures at (near-) normal angle of incidence it is common to only specify the outgoing component.

A parallel set of descriptors exist:

Specular Corresponds to direct in the list above. Originally defined for reflected light, where its meaning is quite the mouthful: the direction light emerges from the reflecting surface which is at the same angle to the surface normal as the incident direction, but on the opposing side of the surface normal in the plane containing the incident and reflected direction. Use of this term for transmittance describes the light propagating in the direction parallel with the incident light. Note that for a

dielectricum with some thickness there is a lateral shift dependent on thickness and angle of incident as the beam is refracted entering the medium and then refracted again exiting the medium, but that light is still considered specular.

Diffuse Corresponds to diffuse or diffuse only depending on context.

Total Corresponds to hemispherical, i.e. the sum of diffuse and specular.

This second set benefit people who only want to use a single letter to differentiate between specular (s) and diffuse (d) whereas the first set requires three letters for dir and dif. However, the effort saved there is probably cancelled out for all the times spectral and specular has been confused or misspoken.

A third way to describe the direct or specular component is using the word *collimated*, pertaining to a beam of parallel rays.

When emissivity is mention in the thermal IR range it there is also a differentiation between direct and hemispherical. While technically true that it describes the outgoing hemisphere, as radiation is emitted from the surface, it should be noted that the absorption is decribed with respect to direct or hemispherical incident illumination.

While not showing up in this report, it is worth mentioning *retro-reflection*, which specifies the light reflected back in the direction of the source. Experimental and practical uses typically includes a limited solid angle defined by the instrumentation.

2 Samples

The ILC was a parallel ILC, i.e. all participants get their own set of samples. This has proven valuable in the past for the participants since they can go back and remeasure their samples after moving or modifying their measurement equipment.

2.1 Sample selection

The sample selection was carried out by the NFRC diffuse glazing task group. A total of six samples were selected from four companies, Viracon, Eastman, Guardian and NSG Pilkington. Vitro formerly PPG provided Starphire® low-iron glass substrates for building the Eastman samples.

1. Diffuse interlayer between two 6 mm low-iron provided by Eastman&Vitro
2. Coated fritted glass provided by Viracon
3. Acid etched 12mm glass provided by Guardian
4. Diffuse applied film provided by Eastman&Vitro
5. Small inverted pyramid pattern on 6 mm glass provided by NSG Pilkington

6. Coated patterned glass provided by Guardian

The first four samples all have homogeneous surfaces that are covered by the standards. Sample 5 and 6 both have inhomogeneous surface but were included to determine if the standard is too restrictive or if it is appropriately conservative.

Samples 1, 3, and 4 are common products that should all behave similarly. Sample 2 is more complex as it has a metal coating on top of the rough surface. While this sample was selected to test the measurement of samples with lower emissivity, it should be noted that it does exist as a product and is not a fringe invention only for this activity.

2.2 Variation between samples

Direct-hemispherical transmittance and reflectance measurements of each individual sample (25 for each specimen) was carried out at 550 nm as well as 1500 nm to give an indication of the sample variation, these measurements were carried out at Guardian (samples 3 and 6 using 270 mm sphere), NSG (sample 5, using 270 mm sphere), Eastman (samples 1 and 4, using 270 mm sphere), and at LBNL (sample 2, using 270 mm sphere) before samples were grouped in boxes and shipped out.

Each sample was measured in three different spots of the surface and averaged. This reduce the impact of any inhomogeneity of each individual sample in this measurement of the variation from sample to sample.

At LNBL the transmittance was measured in time drive for 20 seconds with the signal sampled every second, a typical variation in reading over 20 seconds was ± 0.002. The difference between samples and the average was calculated by subtracting the mean from each measured value. The extreme values as well as the standard deviation is shown in figure 1.

Some points of concern, T(550nm) of sample 2 had the extremes at 0.378 and 0.418, and one standard deviation at 0.01 around 0.39. Sample 4 had over 0.01 difference between min and max but with a standard deviation of 0.005. Other than those results the difference between min and max for transmittance was lower than 0.01. For reflectance it was those two samples that also had the greatest variation, more than 0.01 difference between min and max but still a standard deviation of 0.005 or less.

It is not trivial to conclude what the best action to take is based on this information. Digging into the details of the premeasurements for sample two shows that five specimens of sample 2 studied in this report had a transmittance value at 550 nm centered around a mean of 0.387 with a maximum of 0.3940 and a minimum of 0.3783. That range is significantly narrower than the range shown for sample 2 in figure 1a).

Looking at the complete submission when approving a participant is necessary rather than failing them on a single sample. Running the ILC with a single sample set, which increases risk of damaging the samples in handling and shipping, is far from guaranteed to resolve this issue. Keeping the variation in mind for when comparing the measured spectra is at least something that can be done.

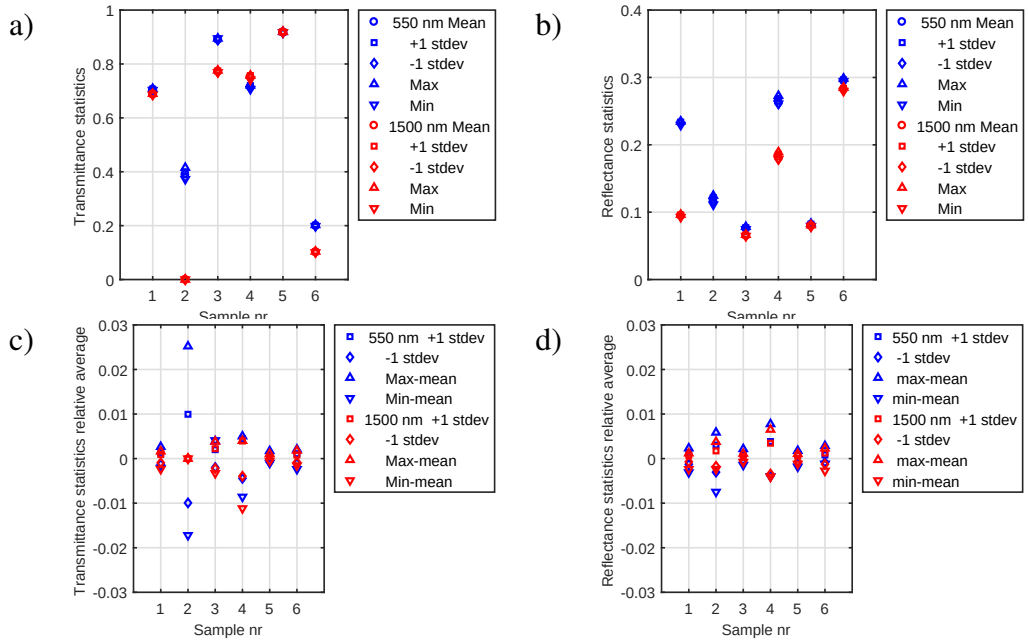

Figure 1: Statistics of the absolute variation of a) transmittance and b) reflectance measured at 550 nm (blue markers) and 1500 nm (red markers) nm for the different samples. In c) and d) the y-axis is arranged so that 0 marks the average for each individual sample.

After the variation had been measured by the manufacturers or at LBNL, the samples where packaged, shipped, and upon reception cleaned by the recipient before they measured it with their instrument.

3 Solar optical range, 300–2500 nm

3.1 Instruments and detectors used

A majority of the ILC participants using a commercial instrument used Perkin-Elmer Lambda 900/950/1050 instruments fitted with a 270 mm integrating sphere for their direct-hemispherical measurements, but a few participants used custom-built integrating spheres (e.g. Fraunhofer ISE with a 620 mm diameter sphere) instead which in the past has been the only option. For sphere that do not have exclusion ports, the specular component was calculated from direct-hemispherical and direct-diffuse measurements with a smaller sphere according to NFRC 300.

The low number of other instrument types limits the ability to draw conclusions from the results in this preliminary report but as more measurements come in this can be updated.

The typical detector combination is a photomultiplier tube (PMT) for the visible range and a lead sulfide (PbS) or an indium gallium arsenide (InGaAs) for the NIR. Older Lab-

sphere 150 mm spheres are fitted with the PbS and more modern 150 mm spheres and the 270 mm spheres are fitted with the InGaAs.

As more results come in this section can be expanded if a greater variation of instruments are used.

For thermal IR emissivity measurements there was also a limited selection, two labs used the Devices and Services AE-1 emissometer, one participant used a INGLAS TIR 100-2 emissometer, and finally one laboratory was using an FTIR fitted with an integrating sphere.

The low-e coated rough surface was sent to two additional measurement labs that could measure spectrally resolved IR reflectance.

3.2 Example of results

There are eight spectra in the data file for each sample from each participant. The number eight is built up through all the combinations of the three pairs reflectance/transmittance, front/back, and direct/diffuse. Attempts to visualize the full set has been considered too busy and instead we are exploring using graphs that only show the data needed for the point that is being discussed in the text. The derived properties haze and hemispherical also come into play which add even more spectra that can be useful to understand the data.

Two examples of the wavelength resolved data is shown in figure 2. The results of a single participating lab, described by box number, are shown in the graphs as solid lines and these results are compared to the dashed line which is an average of all results (discounting outliers). Each participant will get this kind of result for all their samples.

In figure 2a) the diffuse and specular transmittance are shown for sample 1. The specular and diffuse results are reported in the data files submitted. When there is agreement in both those spectra that also means that the total transmittance as well as the transmittance haze are in good agreement. Displaying the submitted data makes it easier to understand what might be wrong or different for a specific lab than looking at the total transmittance and haze. The latter properties are definitely more useful as performance metrics of a product.

In figure 2b) reflectance, transmittance and absorption are all displayed. As sample 2 has different front and back properties there is a clear difference between the front and back reflectance.

3.3 Normal-hemispherical visible and solar results

This section presents average results for all participants, integrated results for all samples with participants broken out are shown in the appendix A. At time of writing this report the results from box 11 were considered outliers, LBNL will work with that lab to try to understand where the issues originate.

While the normal-hemispherical value is not reported it is interesting to review as it relates to the total energy being either transmitted and reflected. Furthermore, it is the

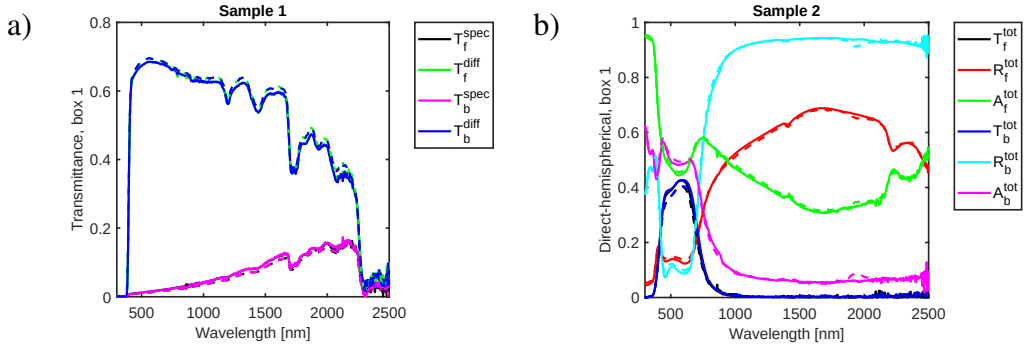

Figure 2: Example of spectral data submitted for box 1 for sample 1 in a) and sample 2 in b). The dashed line is marking the average of non-outlier submissions.

value, that due to the larger sphere, allows characterization of diffuse samples without the systematic errors that are present in the small integrating sphere measurements. It is also slightly more manageable to review four properties before looking at the next section where all eight submitted properties are reviewed.

Figure 3 shows the average normal-hemispherical results and the minimum and maximum reported value for each integrated property. The solar values fall within the specular tolerances (± 0.01 for transmittance and ± 0.02 for reflectance) in all cases except for the front transmittance sample 4 (see appendix A.4 for data of individual participants to see the spread more clearly). The visible values have more entries outside of the tolerances, both for reflectance (samples 1 and 2) and transmittance (samples 2 and 4).

The maximum difference between the average, shown in figure 4, found for each property where at least one participant fell outside tolerance was calculated to give a sense of the magnitude of the issue. For transmittance the largest differences were 0.0127 (Tsol front sample 4), 0.0156 (Tvis front sample 4), 0.0109 (Tvis back sample 4), and 0.0105 (Tvis back sample 2). The reflectance the largest differences were 0.0255 (Rvis front sample 1), 0.0256 (Rvis back sample 1), and 0.0213 (Rvis front sample 2). So, it is interesting to see that increasing the tolerance for transmittance to 0.02 and reflectance to 0.03 would result in all the reported direct-hemispherical values to be within tolerance.

3.4 Normal-normal and normal-diffuse visible and solar results

The data reported for a sample includes 8 values for each wavelength, all combinations of transmittance/reflectance, normal-normal/normal-diffuse, and front/back. This section investigates the average of these properties and the variation from that average between the participants.

Figure 5 shows the integrated solar and visible results for all the properties submitted. Using the same process similar as in the previous section the largest difference from the average was calculated for each sample where the result was outside that of the tolerances used for specular samples.

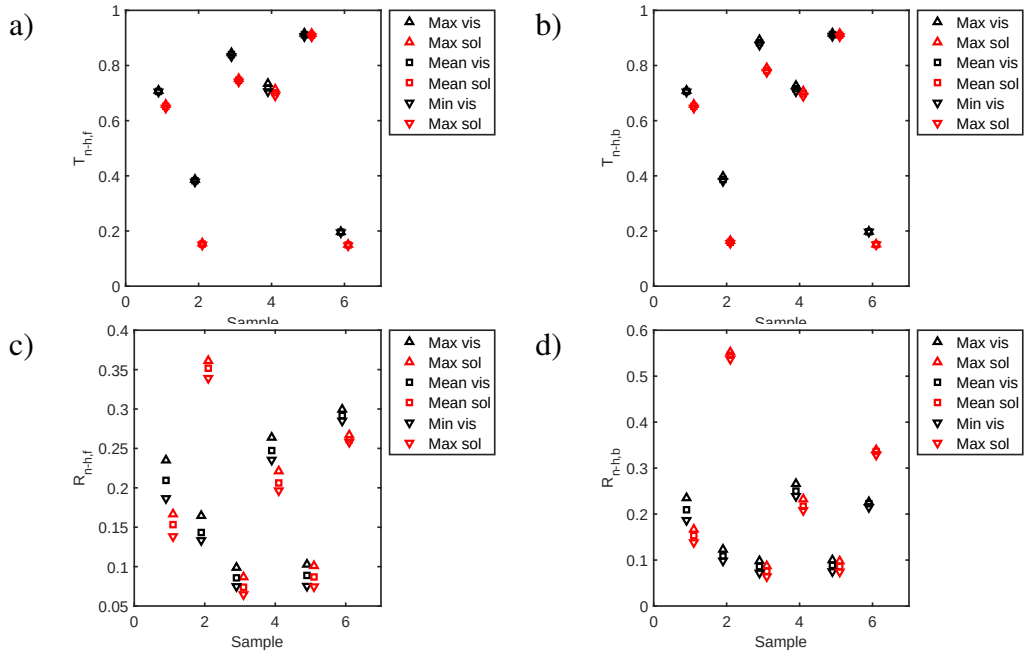

Figure 3: Normal-hemispherical values (y-axis) for all samples (x-axis) averaged between the participants and showing minimum and maximum measure values. The visible and solar values are slightly offset on the x-axis to not cover each other. The property in each graph is a) front transmittance, b) back transmittance, c) front reflectance, and d) back reflectance.

The differences between maximum and minimum for sample 5 and 6 are very large. The difficulty to characterize those samples are further discussed in section 3.5, where it is also explained why those samples are not considered in this section.

For transmittance sample 3 and 4 had results that were outside the tolerance range and for reflectance sample 1 and 2 had results that did not fall in the range. The largest differences between average and participant for transmittance were 0.0274 (sample 4 $Tsol_{n-n,f}$), 0.0231 (sample 4 $Tvis_{n-d,b}$), 0.0230 (sample 3 $Tvis_{n-n,b}$), and 0.0172 (sample 3 $Tvis_{n-d,b}$). For reflectance the largest differences were 0.0383 (sample 2 $Rsol_{n-d,b}$), 0.0352 (sample 2 $Rsol_{n-n,b}$), 0.0220 (sample 1 $Rvis_{n-d,f}$), 0.0220 (sample 1 $Rvis_{n-n,b}$), and 0.0205 (sample 2 $Rsol_{n-n,f}$).

Due to how the n-h, n-n, and n-d results are connected it is reasonable to see issues with both the n-n and n-d values if there is good agreement between the n-h values.

The variation in geometry between different sphere was a cause for concern and a control was put in place to handle that systematic issue. However, despite early partial results showing that it helped it does not look like it is sufficient to get good agreement for all different types of samples. A more detailed study of the scattering distribution and impact of the half-angle of the exclusion port used to obtain the diffuse value is conducted in the next section. Spoiler-alert, the results does not give a direct solution but rather hints

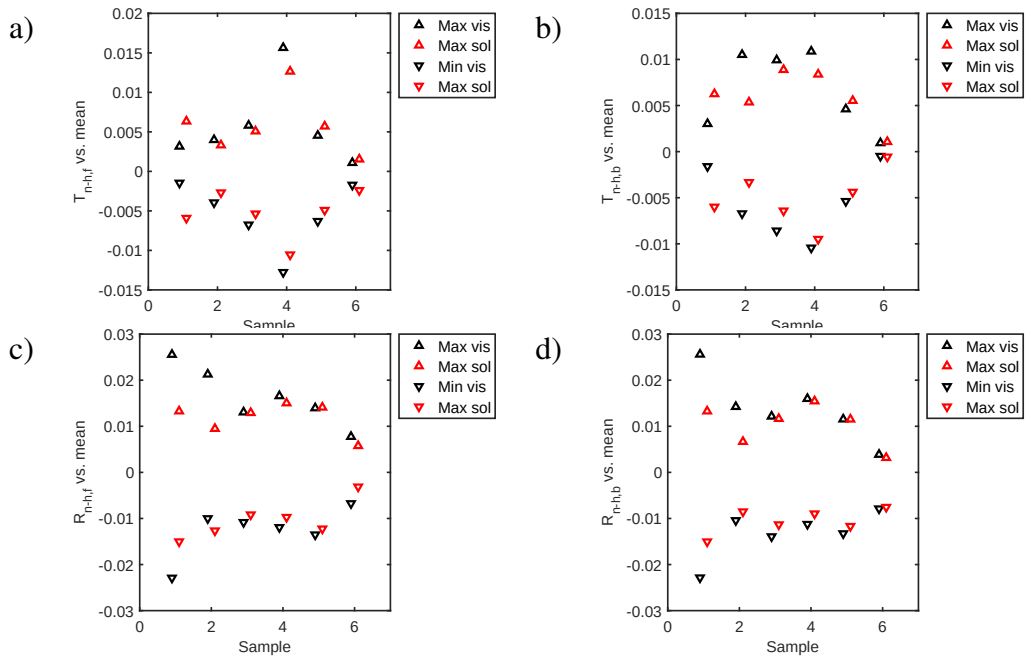

Figure 4: The largest differences from the average for each sample for a) transmittance front, b) transmittance back, c) reflectance front, and d) reflectance back.

at why the control put in place is not a fool-proof correction.

Based on these results it would be necessary to increase the tolerance of the reported transmittance values to ± 0.03 and the reported reflectance values to ± 0.04.

3.4.1 Detailed analysis of normal-normal results

A detailed study of the scattering distribution for the ILC samples demonstrate how the impact vary between samples, based on how the scattering of the samples differ. Bi-directional scattering distribution function (BSDF) data for the samples were obtained using a pgII photogoniometer with a v(Lambda) filter which gives a T_{vis} value. It is possible to predict the specular component for an integrating sphere with any port opening by integrating the distribution up to angle matching the exclusion port.

This method approximates the beam as a point in the center of the port, which is not realistic. The LBNL Lambda 950 with 150 mm integrating sphere has a rectangular beam at the entrance port which is approximately 10 mm by 17 mm in a 25 mm diameter port. So it is reasonable to expect that the edges of the beam do see the port differently than the center.

A way to visualize this calculation is shown in figure 6. The normal-conical description is used for the value on the y-axis, emphasizing that it is a function of the half-angle given on the x-axis. The normal-normal value obtained through integrating sphere measurements should in theory match the T_{n-con} value for the half angle given by the integrating

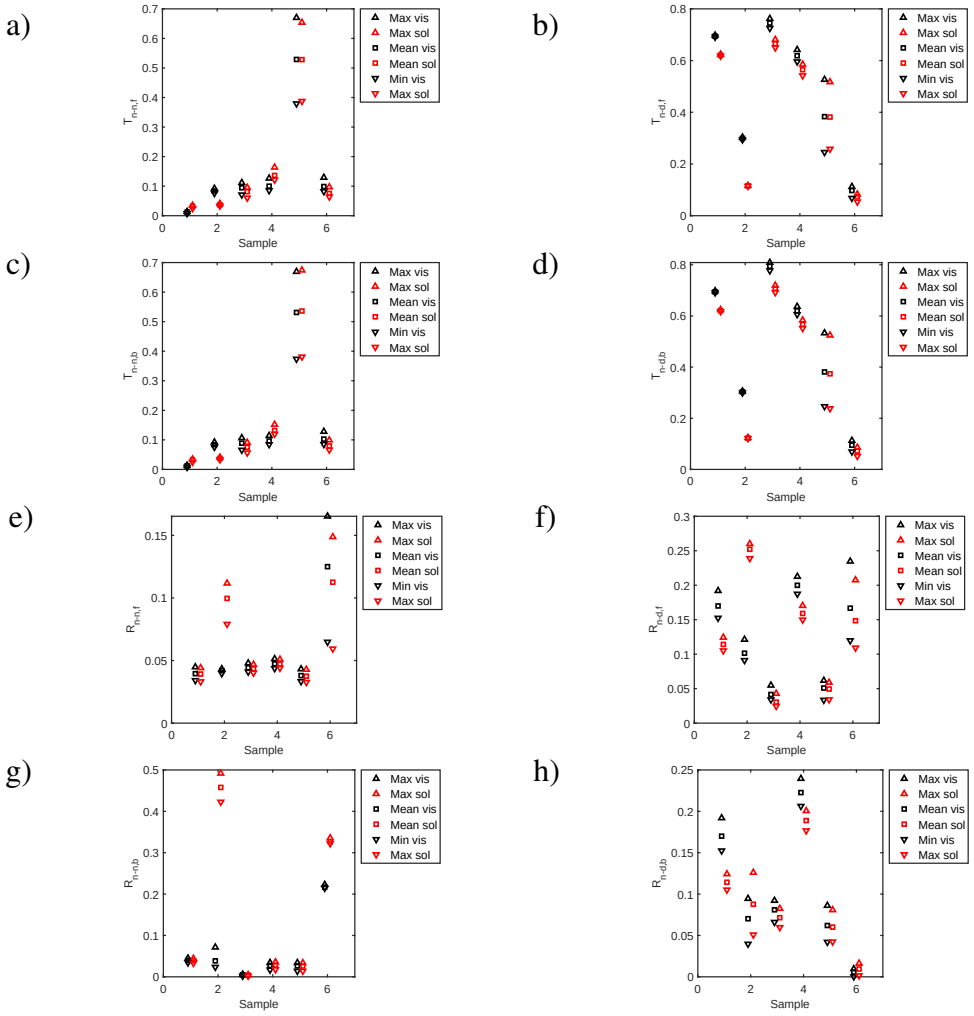

Figure 5: Normal-normal and normal-diffuse integrated values for each sample averaged over all participants with maximum and minimum values included.

sphere geometry.

It is possible to compare this n-con value with the normal-normal value obtained for the angle on the x-axis that matches the half-angle of the scattering cone which corresponds to the geometry of the sphere used. Another comparison is to use the measured n-n value and see what half-angle that corresponds to using the n-con graph. Such a comparison is done in figure 7a).

Figure 7b) shows the relationship between predicted half-angle and the geometrical half angle. The most likely explanation to for the variation is that the approximation that the incident beam is point-like at the center of the entrance port is too crude. The impact of this approximation will depend on the BSDF of the sample as well as the shape and intensity variation of the light spot of the instrument. This adds uncertainty despite the

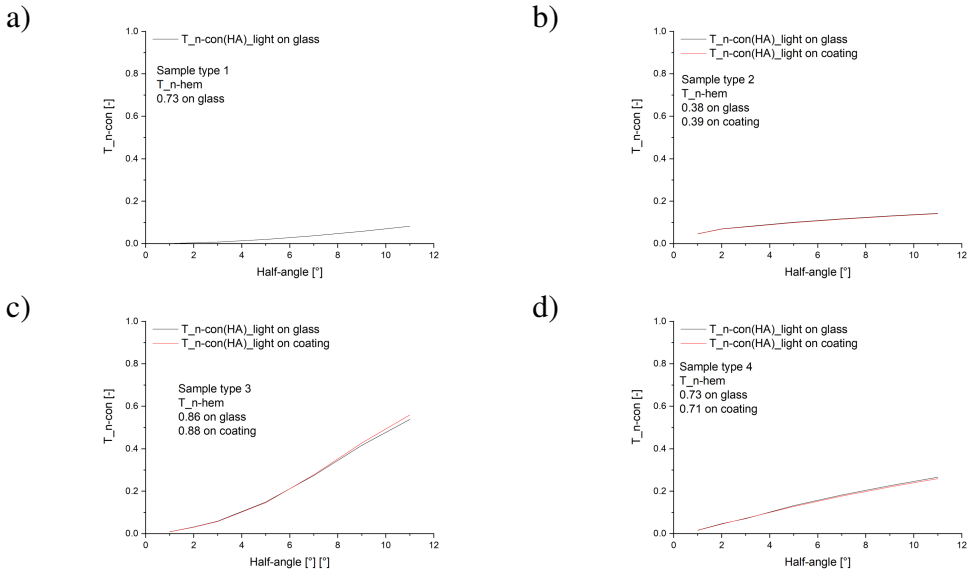

Figure 6: Normal-conical values for samples 1-4 in a) to d), respectively. The visible transmittance scattering distribution function has been integrated in an outgoing direction up to the value on the x-axis. This would match the specular value obtained using measurements with an integrating sphere where the exclusion port matches that angle.

control to do pullback measurements for samples where the derivative of the n-con curve is high around the low half-angles. All of this feeds into the conclusion that a higher tolerance is required for the specular component, which translates to a larger uncertainty in the haze value.

3.5 Issues with samples 5 and 6

NFRC 300 and 301 only allow for homogeneous samples which are isotropically scattering (rotational symmetry of infinite order). Samples 5 and 6 falls outside of these limitations as the inhomogeneities are on a significant scale with respect to the size of the illuminated area, and in the case of sample 6 there is a significant rotational asymmetry.

The positive result is that the direct-hemispherical results were in good agreement. All the visible and solar values show in figure 3 for samples 5 and 6 were within the tolerances for specular samples. Using the large aperture integrating sphere to obtain those values is a valid approach.

However, obtaining good agreement for the specular value requires a more novel approach.

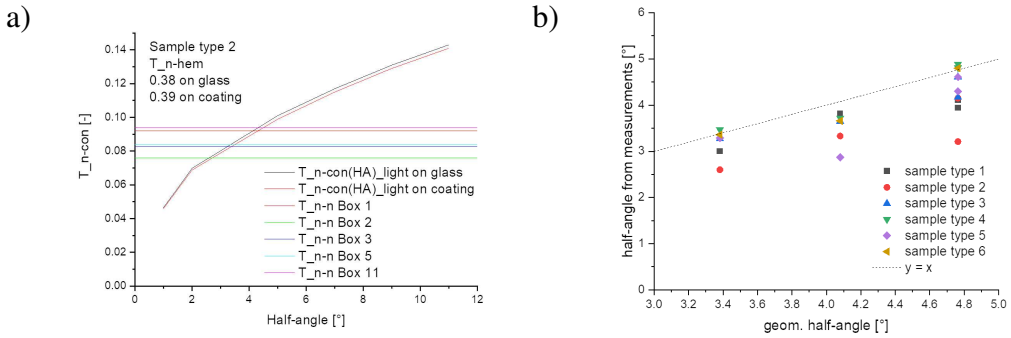

Figure 7: a) The measured n-n value for each participant plotted as a line in the n-con graph for sample 2. The intersection between the line and the curve marks the predicted half-angle geometry of the sphere used by that participant. b) The physical sphere half-angle geometry of the participants on the x-axis. The y-axis has the predicted geometry based on where the measured n-n value intersected the n-con curve.

3.6 Haze

Haze is defined as the ratio between the outgoing diffuse and hemispherical components and it is a simple metric describing how diffuse something is. By that definition haze can be calculated for both reflectance and transmittance as well as for each wavelength which can be integrated to visible or solar results.

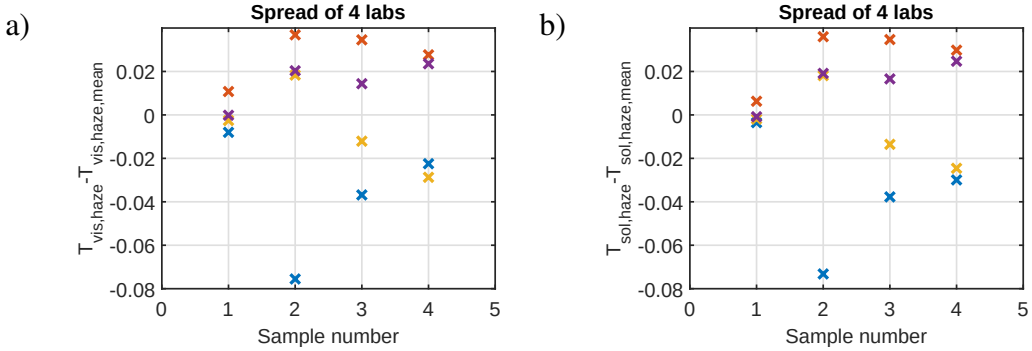

Figure 8: Difference in haze calculated from front transmittance compared to the mean for each participant. In a) the visible integrated value and in b) the integrated solar value.

The visible and solar haze does not have to be identical as shown in figure 8. The variation is greater than seen in the individual values, and a discussion about that general property of haze is found in section 3.6.1. There is also a trend that the blue x (participant one) underestimated the haze for all samples but most significantly for specifically sample two.

This was a concern when NFRC 300 was written. As the division between specular and diffuse light is given by the solid angle defined by the sphere geometry of the instrument,

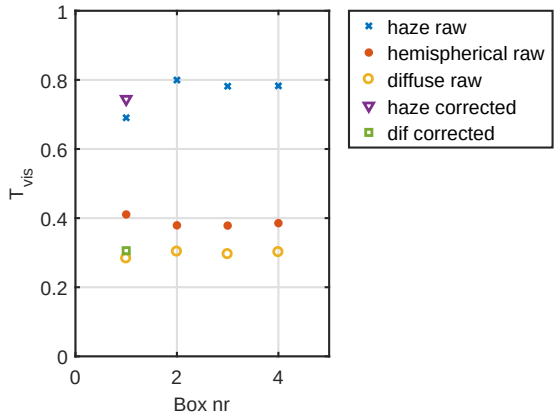

Figure 9: Showing impact on haze value after proper correction of specular value for box 1. A small change in T_{diff} results in a large change in haze value. There is still some difference after the correction, but that is due to the higher T_{hem} value. The transmittance shown is front transmittance for sample 2.

i.e. the size of the specular exclusion port influences how much of the hemispherical value is counted as specular and how much is counted as diffuse.

A method to harmonize results between different sphere designs was included in NFRC 300 and participant one's initial results had interesting diffuse properties that highlighted the need for this. Without repeating the process it specifies a way to get a harmonized direct value. The effective solid angle of the exclusion port is reduced by pulling the sample back from the entrance port of the sphere (hence this method is sometimes referred to as the pullback method). Using that the error in both hemispherical and diffuse measurement is the same, subtracting diffuse from hemispherical gives an accurate direct result.

Participant one (results for box 1), the blue x from figure 8, was using a Labsphere 150 mm sphere without any correction. After remeasuring the specular component using with the sample pulled back 54mm a small increase in diffuse value was seen which resulted in significant increase in the haze value. There is still disagreement between box 1 and the others but that is tied to the higher T_{hem}-value.

3.6.1 Uncertainty in haze

The uncertainty in haze will not be linear to that of the measured values as it is calculated as the ratio between two values. The magnitude of the uncertainty in haze will increase with decreasing values for the hemispherical value, assuming an absolute (rather than relative) uncertainty for the hemispherical value.

Demonstrating this by looking at the definition of haze with respect to the two inde-

pendent values where the transmitted haze can be written as

$$H_T = \frac{T_{n-diff}}{T_{n-hem}} = \frac{T_{n-hem} - T_{n-n}}{T_{n-hem}} = 1 - \frac{T_{n-n}}{T_{n-hem}}. \quad (1)$$

Assuming the uncertainty for T_{n-n} and T_{n-hem} to be ± 0.03 and ± 0.02, respectively, the impact of the magnitude of T_{n-hem} with respect to the uncertainty in haze value can be demonstrated by looking at two results yielding a haze of 0.9.

Case one, with low T_{n-n}, a sample is reported with $T_{n-n} = 0.01 \pm 0.03$ and $T_{hem} = 0.10 \pm 0.02$, the worst case haze values would be $1-(0.04/0.08) = .5$ and $1-(0.0/0.12) = 1$ (ignoring the non-physical edge case of $T_{n-n} = -.02$).

Case two, with a high T_{n-n}, a sample is reported with $T_{n-n} = 0.08 \pm 0.03$ and $T_{hem} = 0.80 \pm 0.02$, the worst case haze values would be $1 - (0.11/0.78) = .86$ and $1 - (0.05/0.82) = .94$.

Understanding that there is a link between haze uncertainty and hemispherical values is helpful when using haze for any kind of decision making or comparison.

4 Thermal infrared range, 5–25μm

Measuring thermal IR data is needed for calculation of the insulating properties of a glazing system (U-value).

4.1 Instruments used

Most instruments used for IR measurement of specular glazing only measure specular reflectance. Such instrument are inadequate for measurement of samples with surface roughness.

NFRC 301 allows using emissometer instruments like the Devices and Services AE-1 for measuring an integrated single value as an alternative to using an integrating sphere.

4.2 Emissivity measurements

Using an emissometer gives a single value for the hemispherical emissivity, and the accuracy is dependent on how well the emissometer is calibrated. In theory the scattering distribution of the references should match that of the measured sample, but most emissometers are only delivered with one set of standards.

The CGDB contains information about the emissivity in the infrared range. To obtain this value reflectance is measured and since the samples are opaque in the infrared wavelength region so the absorption is equal to one minus the reflectance. The spectral absorption is weighted using a 300 K black body curve according to NFRC 301. This temperature is the default in the LBNL Optics/WINDOW programs.

In the preliminary results there where only three labs that reported results are shown in figure 10. The x-axis has each sample and the y-axis has the hemispherical emissivity of

the sample's *treated* surface. The exception is sample one, i.e. the laminate, where both front and back were untreated. The agreement between the three labs were within ± 0.02 for all samples and within 0.01 for sample 2 with the low-e coating.

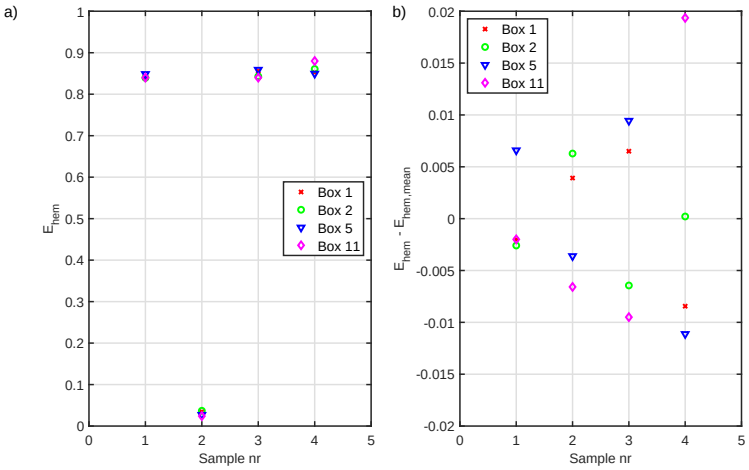

Figure 10: Hemispherical emissivity of the rough sample surface for each sample shown for four labs that submitted IR data. The x-axis has the sample and each lab has its own marker. In a) the actual values for each sample, in b) the difference between each lab and the average of the three.

Values for boxes 1, 5, and 11 were using broadband emissometers (D&S AE-1 and INGLAS TIR 100-2) which only reports a single number. Results for box number 2 were integrated from spectrally resolved data obtained using an integrating sphere.

4.3 Spectral data analysis of rough low-e coating

One question the NFRC Diffuse Glazing Task Group had not answered was the question if the emissometers could be trusted with regards to measuring the emissivity of low-e coated rough surfaces. The sample was measured using three different integrating spheres: LBNL Prasher lab (not the windows group), Optical Data Associates, and Fraunhofer ISE. The spectral result is shown in figure 11.

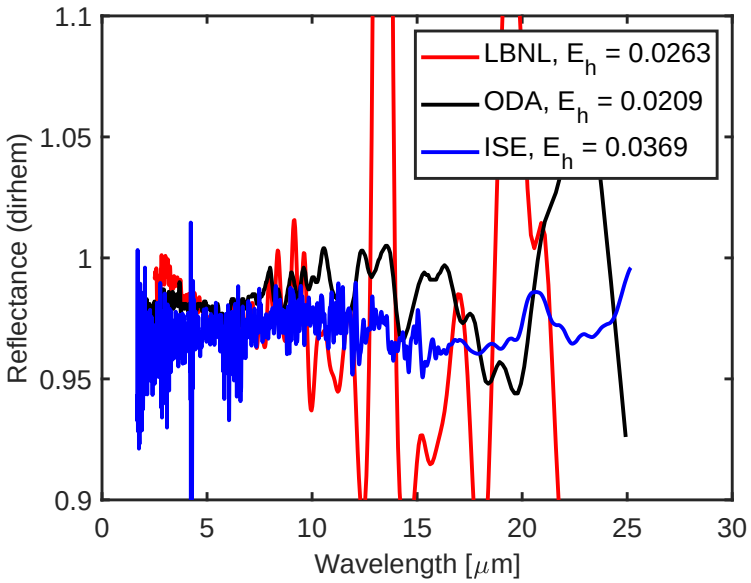

Figure 11: Spectrally resolved reflectance for the coated rough surface measured using FTIRs fitted with an integrating sphere. The noise above 10 micron is unreasonably high for the LBNL sphere.

The large amount of noise in the LBNL spectrum at longer wavelengths than 10 micron is suspicious. But for this exercise the data between 2 and 10 micron does support the argument that the agreement between emissometer and integrating spheres is good.

Measurements using FTIR instruments fitted with an integrating sphere was carried out to give further confidence in the measurement of the low-e coated rough surface (sample 2). The average E_h for sample 2 using only emissometer measurements was 0.0285 and including the three integrating sphere measurements the average is 0.0283. The integrated hemispherical emissivity calculated from spectral data agree well with the data from the emissometers.

The NFRC 301 method to calculate the hemispherical value from the direct emissivity was used. That method was derived using specular samples, but considering the good agreement between emissometers and integrating spheres there is not yet evidence that it cannot be used for these rough samples as well.

5 Validation of WINDOW 7.8 using diffuse data

WINDOW 7.8 has the possibility to perform multilayer calculations of diffuse layers with spectral data that can be imported into the CGDB. Testing this capability was carried out and the results are shown here.

5.1 Common parameters

The WINDOW preferences that were switched from default are all present in the **Optical calcs** preference tab. The **Spectral data** option was set to *Condensed spectral data* with 5 visible bands and 10 IR bands. The **Angular basis** used was *W6 standard basis*.

Some tests on specular samples were carried out with the **Use matrix method ....** option checked to show the impact of using the condensed spectral data instead of the full spectrum.

5.2 Samples used

Data in the direct-diffuse CGDB data format can be imported in WINDOW shading library and were used for the testing in addition to IGDB entries already in the database. This is the same file format that was used for data submission in the ILC.

clear3 The IGDB entry for Clear_3.dat NFRC ID 102, glass layer

solarban The IGDB entry for Solarban 70_6.VTA ID 5439, oriented so that the coated surface is towards the cavity, glass layer

clear3spec CGDB file with Clear_3 data in the specular columns, no diffuse component, shade layer

solarbanspec CGDB file with solarban data in the specular columns, no diffuse component, shade layer

clear3diffonly CGDB file with Clear_3 data in the diffuse columns, no specular component, shade layer

solarbandiffonly CGDB file with solarban data in the diffuse columns, no specular component, shade layer

ILC1 CGDB file with data for ILC sample 1, diffuse interlayer laminate, shade layer

ILC2 CGDB file with data for ILC sample 2, fritted glass with low-e on the fritted surface, shade layer

5.3 Compute time

The computation time is highly tied to the performance of the computer used to run WINDOW. A few examples of glazing system calculations are given here to demonstrate that it is slower than the regular specular calculations. The calculation time increase of visible and solar integrated properties is seen in other computations with a scattering layer, e.g. Venetian blinds, and is not specifically tied to the new diffuse glazing model.

Three different calculations were performed using the clear3 as glass layer 1 (outer) and solarban as glass layer 2 (inner).

For standard specular calculation the task takes less than 2 seconds. With a condensed wavelength band, 5+10 bands = 17 wavelengths, the multilayer calculation for all wavelengths took 13 seconds and the spectral average calculation of visible and solar properties took an additional 2 minutes 20 seconds.

For full spectral, 477 wavelengths, the multilayer calculation took 6 minutes and 10 seconds and the spectral average calculation again took an additional 2 minutes 30 seconds.

5.4 Specular test cases

The first test series use IGDB spectral data for both layers and force WINDOW to use the matrix multiplication calculation to see the impact of the conversion to Klems matrix. This matrix calculation was carried out both with full and condensed spectral data to highlight the accuracy of the condensed method. The results are shown in table 1.

Test nr	Glazing system	Calculation method	Tvis	SHGC	U-value
1	Clear3+Clear3	Specular	0.814	0.763	2.73
2	Clear3+Clear3	Matrix, full spectral	0.814	0.763	2.73
3	Clear3+Clear3	Matrix, condensed	0.811	0.762	2.73
4	Clear3+Solarban	Specular	0.653	0.358	1.626
5	Clear3+Solarban	Matrix, full spectral	0.653	0.358	1.626
6	Clear3+Solarban	Matrix, condensed	0.641	0.354	1.626

Table 1: WINDOW 7.8 calculation using specular IGDB data and comparing the matrix calculations with condensed and full spectral data with the standard specular calculation method. The discrepancy in Tvis and SHGC was less than 0.01 when going to condensed full.

The agreement is excellent between the specular and the full spectral matrix calculation. Going to the condensed spectrum does introduce a difference in the integrated values, with a larger impact on the system with the selective coating.

The second test is used to verify that a diffuse data file with only specular component gets the same result as when using the IGDB data. The results are shown in table 2.

Test nr	Glazing system	Calculation method	Tvis	SHGC	U-value
7	Clear3+Clear3spec	Matrix, condensed	0.811	0.761	2.73
8	Clear3spec+Clear3spec	Matrix, condensed	0.811	0.761	2.73
9	Clear3+solarbanspec	Matrix, condensed	0.641	0.354	1.626
10	Clear3spec+solarbanspec	Matrix, condensed	0.641	0.354	1.626

Table 2: WINDOW 7.8 calculation using dir-dif data file with data in the specular columns only. Doing multilayer calculation both with a mix of glass layer+ shade layer (case 7 and 9) and the same data but as two shade layers (case 8 and 10).

The reason for the SHGC not being identical between case 3 and cases 7 and 8 is due to rounding errors splitting the transmittance and reflectance values up into the Klems patches and then reassembling the result at the end. This error is small and for all the Tvis as well as the SHGC calculation of cases 9 and 10 there was agreement down to at least 3 decimals.

5.5 Diffuse test cases

Data files with diffuse-only data was created using clear3 and solarban spectral properties, and the results using those are shown in table 3. Scattering the light all over the hemisphere should change the result as light will be incident at a wide range of angles instead of only at normal. However, using the same spectral data there should be similar to the specular case.

Test nr	Glazing system	Calculation method	Tvis	SHGC	U-value
11	Clear3spec+Clear3diffonly	Matrix, condensed	0.814	0.764	2.73
12	Clear3spec+solarbandiffonly	Matrix, condensed	0.643	0.359	1.626
13	Clear3diffonly+Clear3diffonly	Matrix, condensed	0.751	0.708	2.73
14	Clear3diffonly+solarbandiffonly	Matrix, condensed	0.567	0.337	1.626

Table 3: WINDOW 7.8 calculation using dir-dif data file with data in the diffuse columns only. In case 11 and 12, both layers are using the shade layers but the first pane has specular component only and the second layer has a diffuse component only. In case 13 and 14 both layer are diffuse only.

Comparing the impact of making the second layer diffuse only is done by looking at case 8 and 11. A very small increase in both SHCG and Tvis is seen (+0.003 in both cases). The scattering of the transmitted light through layer 2 does not change the transmittance, so the root of the increase is due to the reflectance at surface 3 being scattered so that the multiple reflections between layer 1 and layer 2 increases slightly. The visible front reflectance decreases with the same .003 number. The change in angle also increases the absorption for the case with a diffuse layer 2 but for clear glass that number was less than 0.001 for both layer 1 and 2. The effect is amplified when comparing case 9 and 12, which

is not surprising since the reflectance of the low-e coating is much larger. Front reflectance is decreased and balanced by an increase in absorption and transmittance.

5.6 ILC sample test cases

Data files were generated using data from measurements of ILC samples 1 and 2 as examples with a realistic mix of specular and diffuse components. Test cases demonstrating using them as single pane, and in different combinations with other layers were performed.

Test nr	Glazing system	Calculation method	Tvis	SHGC	U-value
15	ILC1	Matrix, condensed	0.694	0.707	5.664
16	ILC2	Matrix, condensed	0.409	0.218	3.145
17	clear3+ILC1	Matrix, condensed	0.637	0.673	2.671
18	clear3+ILC2	Matrix, condensed	0.371	0.277	1.813
19	ILC1+ILC1	Matrix, condensed	0.470	0.529	2.621
20	ILC1+ILC2	Matrix, condensed	0.258	0.226	1.789
21	ILC1+solarban+ILC2	Matrix, condensed	0.171	0.200	0.936

Table 4: WINDOW 7.8 calculation using data from the ILC samples as single layers as well as in different multi pane configurations

There is no gold standard to compare numbers for the test cases with the ILC samples. However, the trends on the three main metrics for glazing do show reasonable results when adding a clear 3 layer. Test cases 19-21 were included to demonstrate that the stack of layers is not limited to having specular layers at any point and there is no limit to only have a maximum of 2 layer.

5.7 WINDOW 7 validation result

This suit of test cases shows no errors in the implementation. However, there are multiple settings in WINDOW that allows to trade accuracy for speed, and knowing when that trade is acceptable or not is not trivial.

Accuracy decreased when using condensed spectral bands instead of full spectral and examples for the magnitude of this difference for a clear and a coated layer. The reason to use condensed spectrum is purely for the calculation speed increase discussed in section 5.3. It is recommended to use the full spectrum calculation instead of condensed if time allows. The loss of accuracy is tied to the spectral variation in the samples so it is more important to use full spectrum for window calculations with spectrally selective layers. Note that this inaccuracy is not directly tied to the matrix calculation process, but since the matrix method is slower, reducing the wavelength resolution is a way to balance calculation time.

6 Conclusions

The low number of participants slightly dampens the confidence in the result, but with both two custom instruments in the mix as well as two instruments using the commercially available 270 mm sphere it looks good. This work allowed for the development of diffuse glazing tolerances as summarized below, and it is recommended to add these tolerances to NFRC 302[3].

For the four isotropic samples the normal-hemispherical solar integrated values were in good agreement, almost within the same tolerance used for specular samples. For the derived values of normal-normal and normal-diffuse reflectance and transmittance the results exceeded tolerances used for specular samples. The complexity of getting agreement in consistently measure the normal-normal value between different instrument was investigated in detail. The same agreement as is seen between specular samples was not obtained despite putting a control in place to harmonize between different sphere geometries. An increase in tolerance for normal-normal and normal-diffuse values of scattering samples is recommended considering the complexity of the property measured and that it is derived from multiple measurements. Based on these results it looks reasonable to increase the tolerance of the reported transmittance values to ± 0.03 and the reported reflectance values to ± 0.04. Furthermore, the good agreement in normal-hemispherical values allows for a tolerance in those values of ± 0.02 and ± 0.03 for transmittance and reflectance, respectively.

The thermal IR hemispherical emissivity was within the NFRC 302 range of ± 0.02. Agreement between FTIR measurements with integrating sphere and emissometers was good even for the low-e coated surface. Based on that finding it is recommended to remove the language in NFRC 301 restricting use of emissometers to a certain emissivity range.

One issue highlighted is the sensitivity of the haze metric with respect to the hemispherical value. As the haze value is very sensitive for low hemispherical values it might be risky to use it independently of the hemispherical value.

WINDOW 7 has implemented the needed calculation procedures to get performance properties from systems with spectral data with direct and diffuse components. The procedure to simulate windows with a diffuse glazing element should be included in the relevent NFRC documents, including the simulation manual.

Special care will be taken when qualifying future participants in this ILC. The large span between the most extreme specimens of sample two for the transmittance at 550 nm could make it hard for a new participant to qualify. If that is the only sample that is problematic, and there are no systematic issues with the result, the submitter shall still be approved.

During the review of this report in the NFRC diffuse glazing TG there are several topics that have been discussed. Unforunately they fell outside of the scope of this work, but are still documented as interesting ideas.

- Grouping of products with similar haze. As the extra work to determine the specular component is significant it would be valuable to quantify the impact of grouping of

products with the same scattering component (e.g. the same diffuse interlayer) but otherwise different components such as substrates or additional specular coatings. What would the impact be of assuming the wavelength-dependent haze is identical for different configurations? Getting real world data from manufacturers measuring this type of sample groups will make a strong foundation for research into this topic.

- It would be interesting to see how the impact of the direct-diffuse model implemented in WINDOW impacts SHGC for different window compositions compared to using actual BSDFs measured using goniophotometers. This would encompass both the angular outgoing distribution and the incident angle properties.

7 Acknowledgement

This work was financed by NFRC. It was supported by the Assistant Secretary for Energy Efficiency and Renewable Energy, Building Technologies Program of the U.S. Department of Energy under Contract No. DE-AC02-05CH11231.

Viracon, Eastman, Vitro formerly PPG, NSG Pilkington, and Guardian assisted with providing the samples that were used.

All ILC participants contributed significant time in measuring the sample properties and resolving issues with the data.

The members of the NFRC Diffuse Glazing TG provided invaluable feedback and greatly helped improve the contents of this report.

References

[1] National Fenestration Rating Council, "NFRC300-2020[E0A0]: Test method for determining the solar optical properties of glazing materials and systems," 2020.

[2] National Fenestration Rating Council, "NFRC301-2020[E0A0]: Standard test method for emittance of glazing products," 2020.

[3] National Fenestration Rating Council, "NFRC302-2020[E0A0]: Verification program for optical spectral data," 2020.

A Graphs for all UV/Vis/NIR results

The graphs on following pages all show integrated solar and visible optical properties for each sample. The individual markers (squares and circles) show reported values and dashed lines show limits imposed by NFRC 302 for specular (.01 for transmittance and .02 for reflectance).

A.1 Sample #1

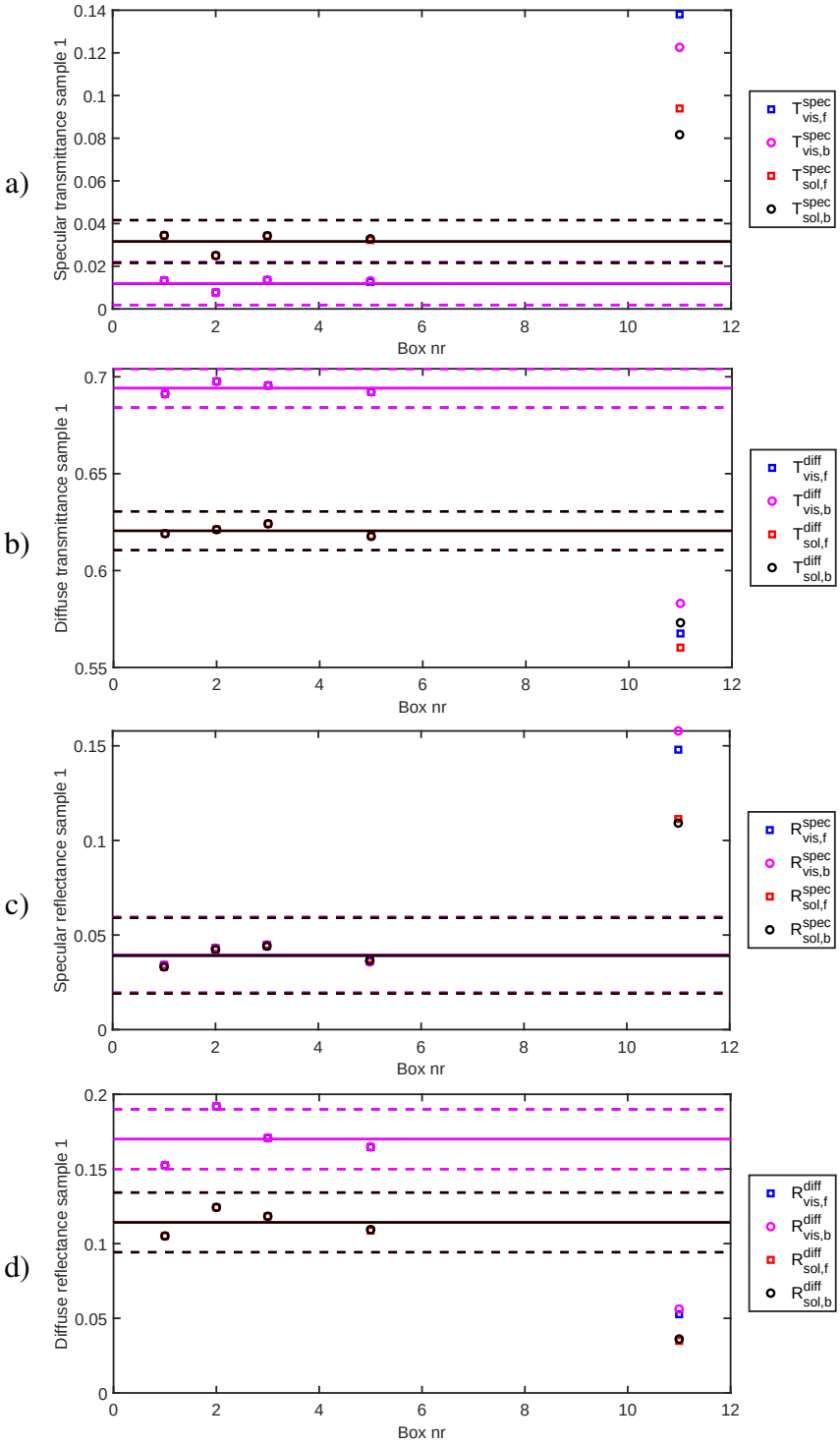

Figure 12: Integrated solar and visible optical properties for sample 1. a) Normal-normal transmittance, b) Normal-diffuse transmittance, c) Normal-normal reflectance, and d) normal-diffuse reflectance.

A.2 Sample #2

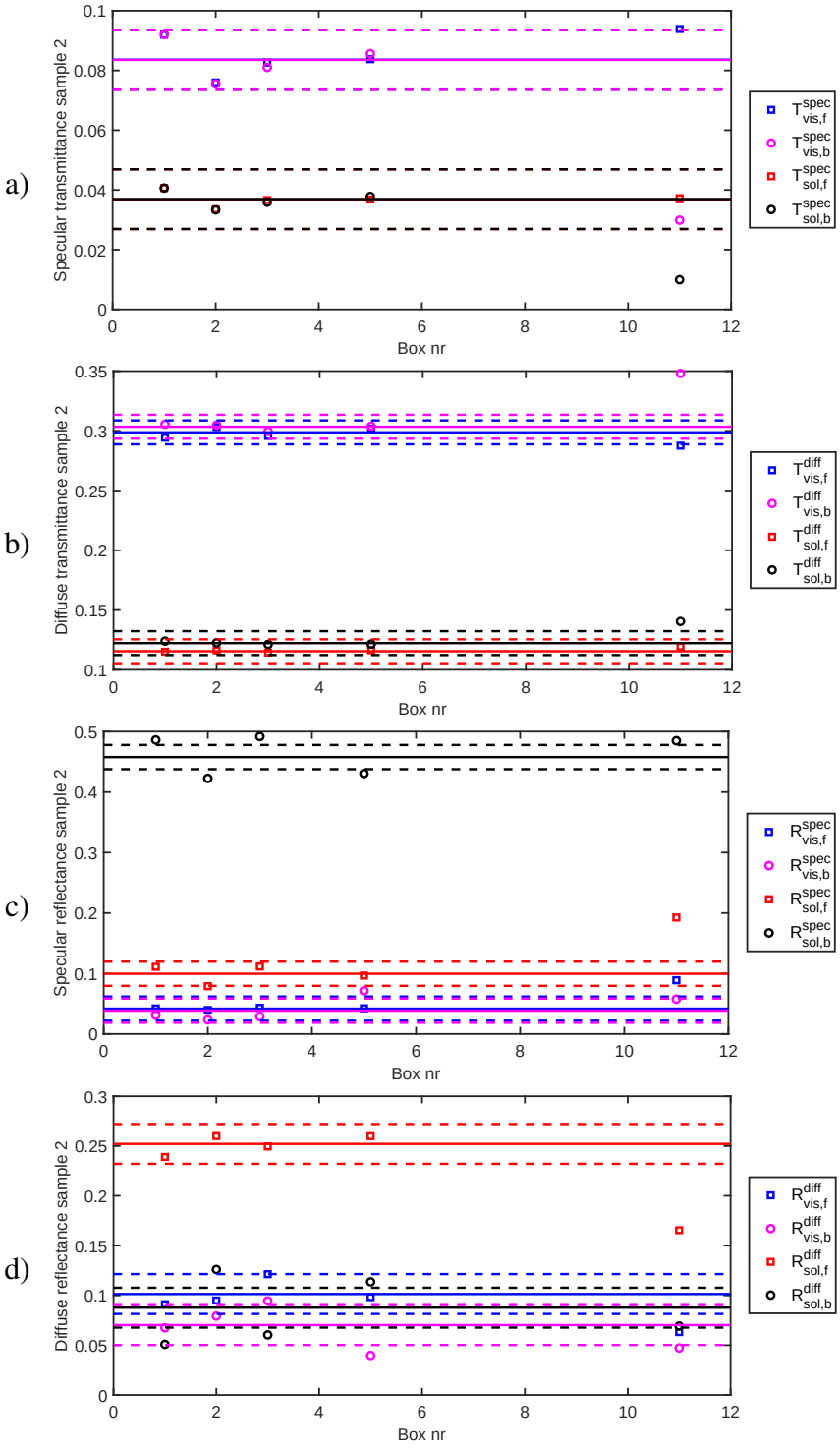

Figure 13: Integrated solar and visible optical properties for sample 2. a) Normal-normal transmittance, b) Normal-diffuse transmittance, c) Normal-normal reflectance, and d) normal-diffuse reflectance.

A.3 Sample #3

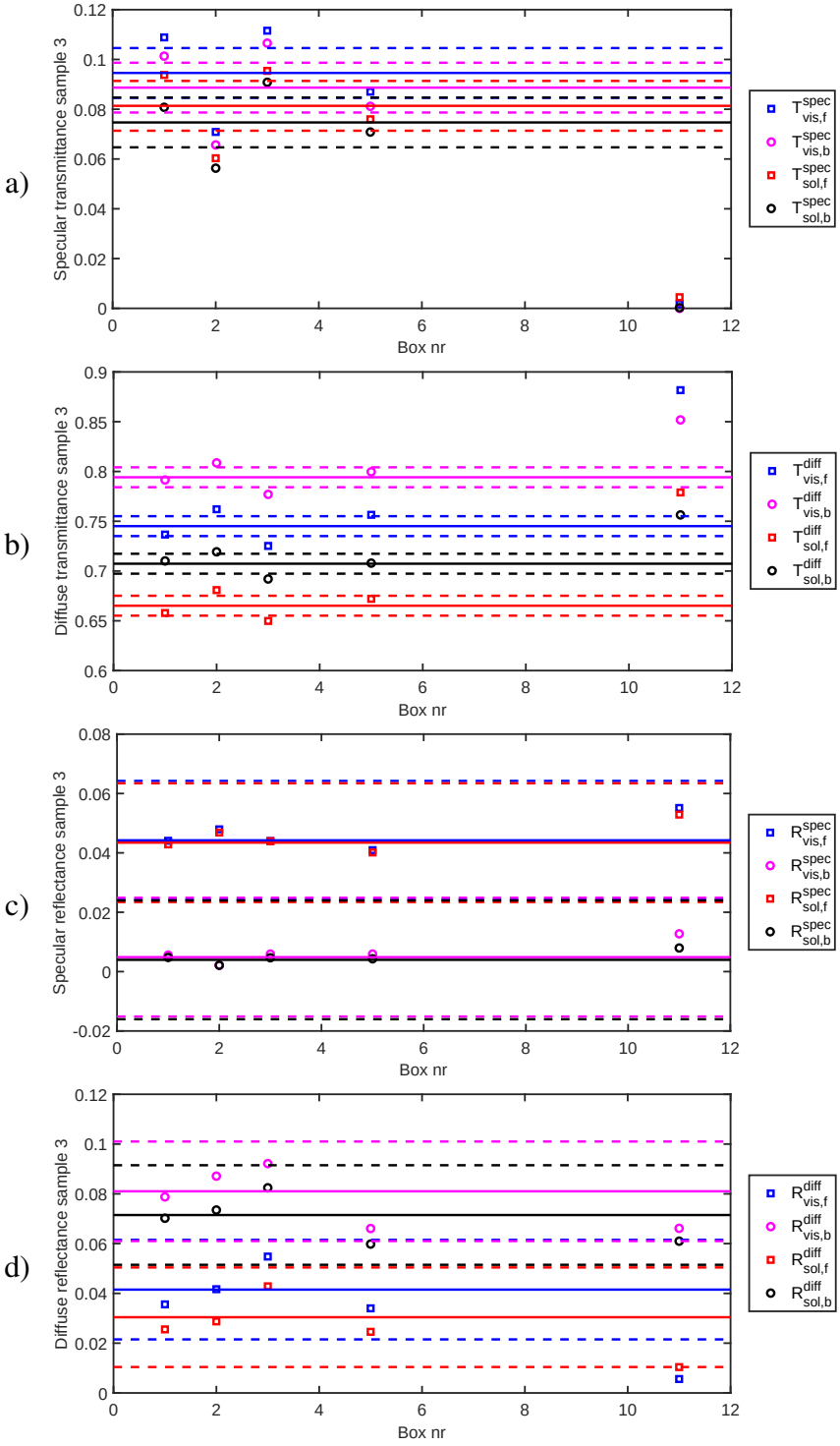

Figure 14: Integrated solar and visible optical properties for sample 3. a) Normal-normal transmittance, b) Normal-diffuse transmittance, c) Normal-normal reflectance, and d) normal-diffuse reflectance.

A.4 Sample #4

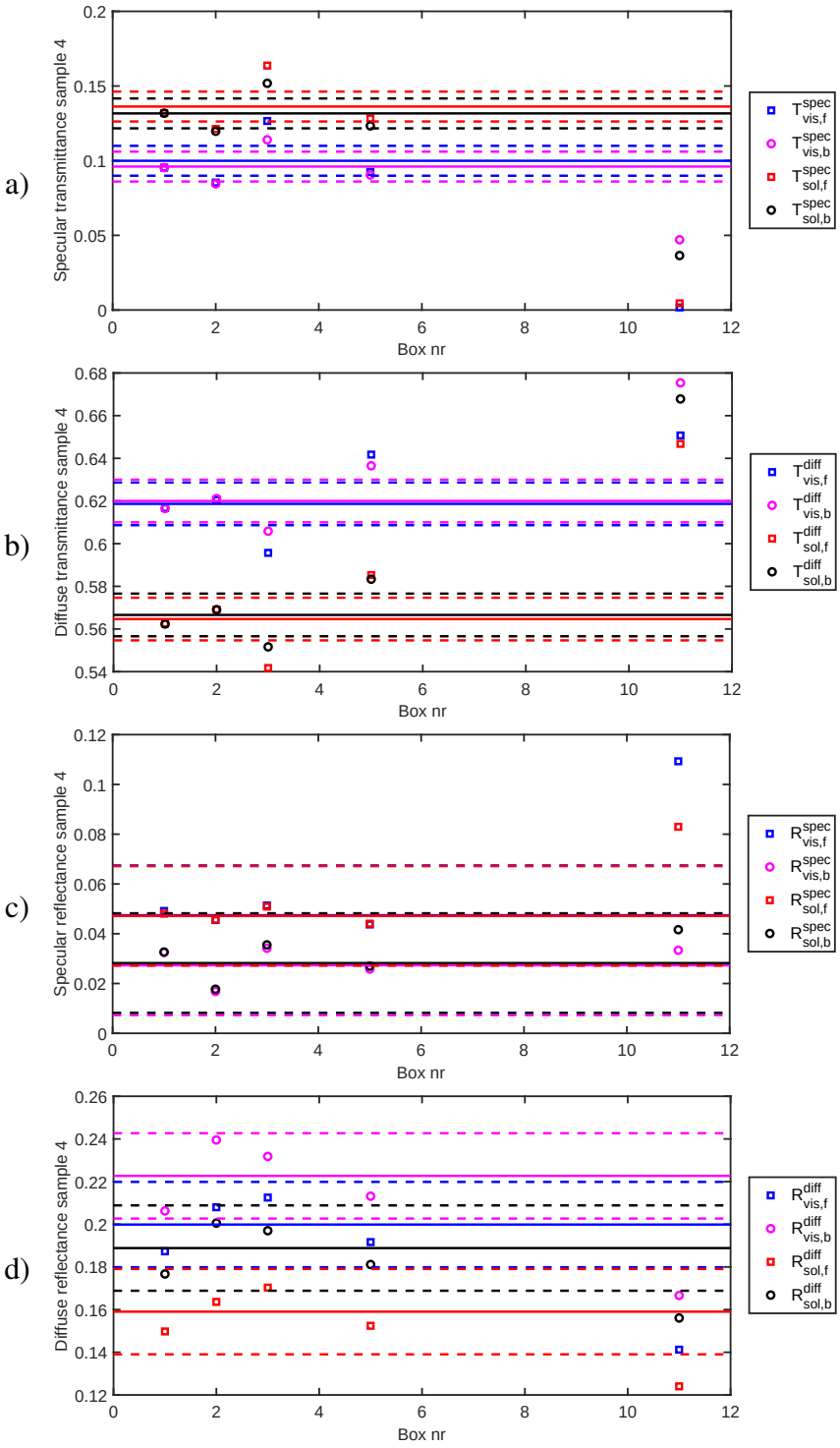

Figure 15: Integrated solar and visible optical properties for sample 5. a) Normal-normal transmittance, b) Normal-diffuse transmittance, c) Normal-normal reflectance, and d) normal-diffuse reflectance.

A.5 Sample #5

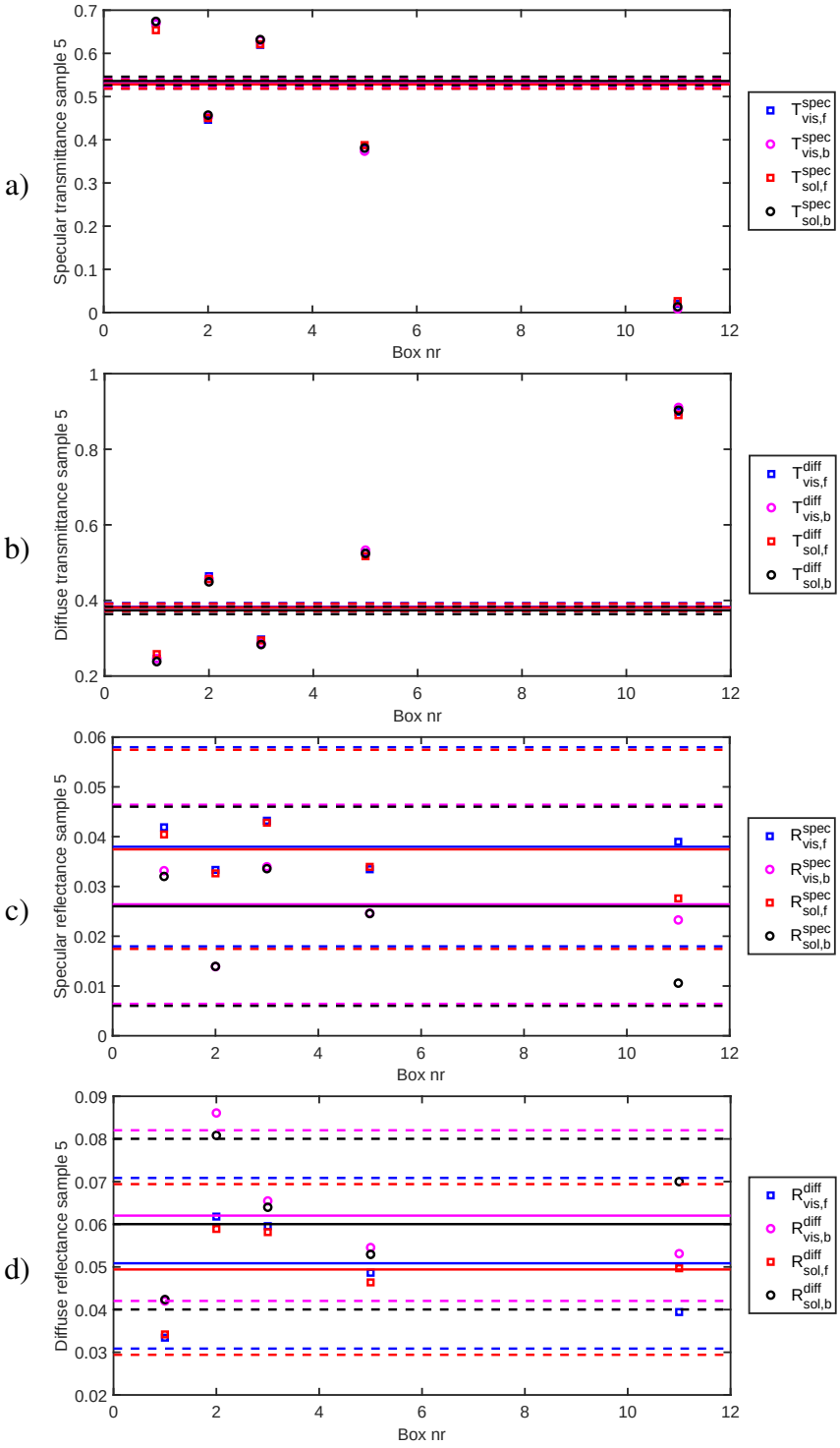

Figure 16: Integrated solar and visible optical properties for sample 5. a) Normal-normal transmittance, b) Normal-diffuse transmittance, c) Normal-normal reflectance, and d) normal-diffuse reflectance.

A.6 Sample #6

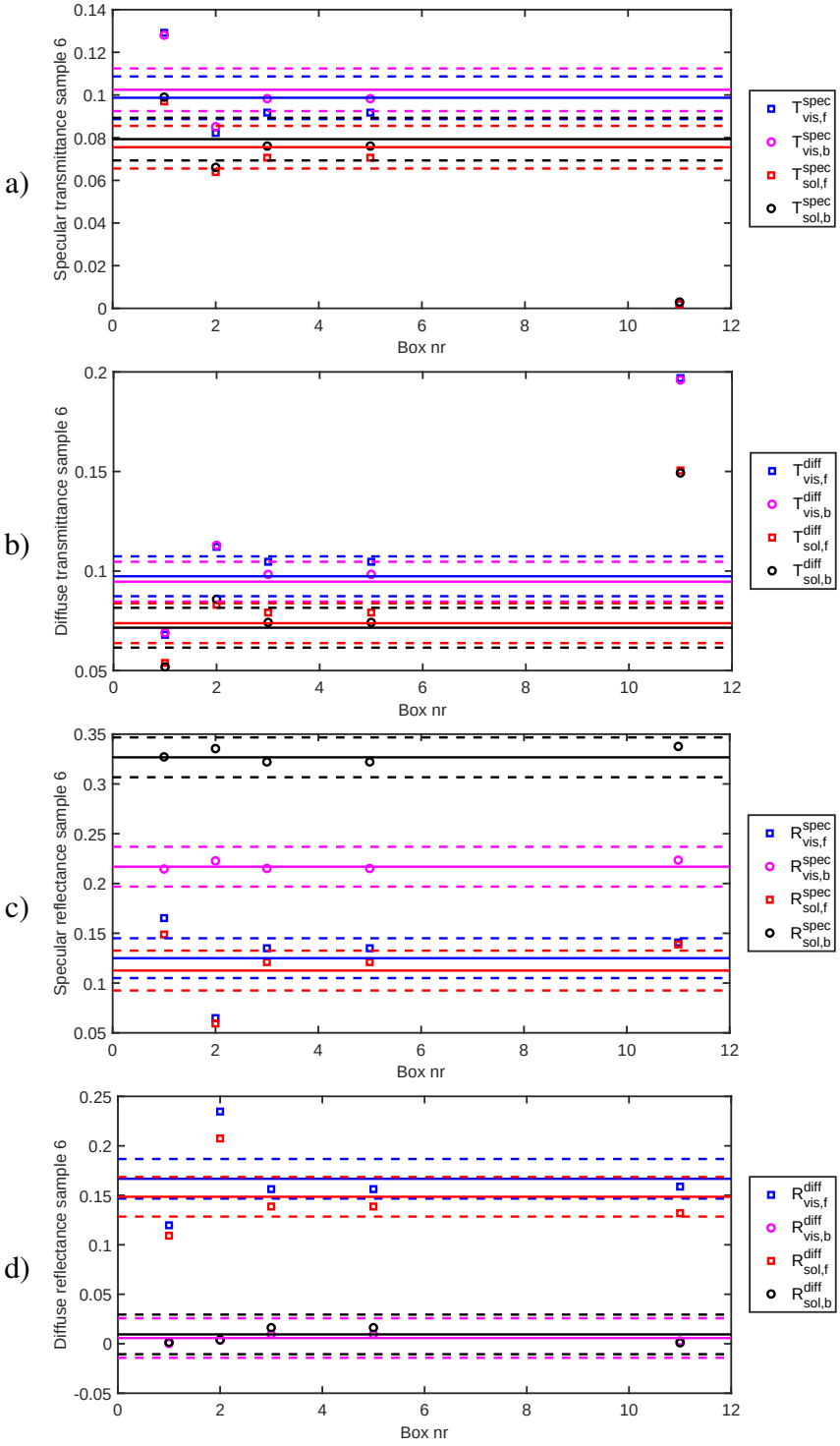

Figure 17: Integrated solar and visible optical properties for sample 6. a) Normal-normal transmittance, b) Normal-diffuse transmittance, c) Normal-normal reflectance, and d) normal-diffuse reflectance.